Ceylon Journal of Science: Physical Sciences, 2(1),35-44 (1995)

FERROELECTRICS DISPERSED Li_2SO_4 COMPOSITE SOLID ELECTROLYTE

K. SINGH and S.S. BHOGA
Department of Physics, Nagpur University, Nagpur-440010, India

ABSTRACT

The feroelectric dispersed lithium sulphate composites have been investigated using complex impedance analysis. The appearence of two semicircles in the Cole-Cole plots is discussed in the light of brick wall model. The observed breakover in the Arrhenius plots within the monoclinic region is considered to be due to changover mechanism from bulk conduction (within grain) to surface percolation conduction. A considerable enhancement in conductivity due to $KNbO_3$ is observed to be due to its ferroelectric property. The surface charge transfer mechanismat the interface is illustrated to understand the formation of a space charge layer and so the microscopic conduction process.

1. INTRODUCTION

Sulphate based solid electrolytes have been extensively studied over a number of years because of their importance in electrochemical devices such as SO_x gas sensors. Lithium sulphate is a well known ionic conductor which undergoes a phase transition from monoclinic to fcc at 848K. In the high temperature fcc phase, it has very high ionic conductivity comparable to those of molten salts[1]. The, low temperature momnoclinic phase is moderately conducting[2].

In past, a number of approaches have been adopted so as to improve conductivity of low temperature phase includes: (i) preparative parameters[3], (ii) aliovalent ion substitution[4,5], (iii) binaries with other sulphates[6] (iv) dispersion of fine alumina particles[7] etc. In many soft-framework electrolytes (e.g. LiI, AgCl, Li_2SO_4 etc.) and in some glasses it has been demonstrated that the presence of insoluble second dispersed phases, in general, insulating phases of hard crystals, in particular, enhances the ionic conductivity[7-11]. Basically, an enhanced conductivity in these systems has been causd by the formation of a highly disordered diffused space charge layer along the interface due to surface interaction and consequently considerable enhancement in ionic transport along the interface has been originally proposed by Jow and Wagner[12] based on the theory of Kliewer and Koehler[13]. Later Maier has elaborated and given an in depth quantitative treatment to these systems[9,14-16]. All above theories point out that the surface charge density and surface activity of dispersoide are the fundamental parameters governing the formation of space charge layer. With these considerations in hand, in one of our studies a considerable rise in conductivity has been achieved by the dispersion of ferroelectric $LiNbO_3$ in Li_2SO_4[17]. Later, Saito et al have studied the effect $BaTiO_3$[18] dispersion in $Na_4Zr_2Si_3O$[12,19]. A theoretical understanding, however is lacking. The

conduction mechanism in such composites is important and can be very well understood using complex impedance analysis. All above factors have evoked much interest to investigate the ferroelectrics and dielectrics dispersed lithium sulphate composites (Li_2SO_4:ABO_3) using complex impedance analysis.

2. EXPERIMENTAL

2.1 Preparation of ceramics:

The dispersoides $BaTiO_3$, $LiNbO_3$, $KNbO_3$ were prepared by conventional solid state sintering of the stoichiometric ratio of initial ingredients (with purity greater than 99.99%) at temperatures 1673, 1373 and 1273 K respectively. Thus obtained ceramics were crushed to obtain the fine particles of micron size.

2.2 Preparation of composites:

Well dried lithium sulphate with 10,20 and 30 wt% of ABO_3 was mixed thoroughly under acetone in an agate mortar. Later, each mixture was pressed to get a pellet of 8mm diameter and 2mm thickness. Finally, the pellets were sintered at 973K for six hours. This technique is similar to that adopted to prepare glass dispersed composite solid electrolytes described earlier[20].

2.3 Impedance measurement:

Prior to impedance measurement, the spring loaded sample was heated to 953K for two hours in order to homogenize the charge carriers in the sample and simultaneously to remove the moisture content therein. Later, the temperature of the furnace was reduced by a step of 293K at the cooling rate of 1K per minute. At the end of each cycle the sample was allowed to attain the thermal equailibrium for dwell time of 60 minutes using an Eurotherm 810 PID temperature controller. During above mentioned cooling process real and imaginary parts of impedance of the sample were measured as a function of frequency in the range from 5Hz to 13MHz and temperature from 953 to 623K at the end of each dwell time as depicted in figure 1 with the help of a computer controlled HP 4192A LF impedance analyzer. HP 16048 test leads were used for electrical connection from sample to analyzer so as to avoid any otherwise parasitic impedance due to improper connecting cables.Entire measurement system was properly shielded. The reproducibility of impedance data was confirmed by repeating the measurements with freshly prepared samples. In order to

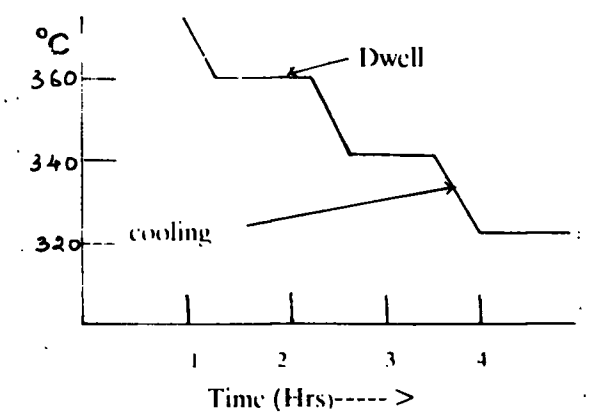

Fig.1 Variation of sample temperature with time

obtain the correct temperature of sample, the tip of a precalibrated chromel/alumel thermocouple was kept in close proximity of the sample. The emf of the thermocouple was measured using Keithley 617 electromerer. The transport number was determined by Wagner dc polarization method with the help of Keithley 236 source measure unit.

3. RESULTS AND DISCUSSION

A detailed analysis of X-ray powder diffraction patterns confirmed the fiormation of pure $LiNbO_3$, $KNbO_3$ and $BaTiO_3$ (ABO_3). Similarly, the X-ray powder diffraction and SEM studies on Li_2SO_4-ABO_3 composites as discussed ealier[20] ruled out the possibility of formation of either any solid solution or intermediate phases.

3.1 Impedace Analysis

The complex impedance plots for pure Li_2SO_4 at various temperatures are shown in figure 2a-c. At higher temperatures (853K) only an inclined straight line is observed. In the temperature range from 813 to 713K a single depressed semicircle follwed by an inclined straight line are seen. The semicircle, however, does not pass through the origin. As temperature reduces further (less than 713K), in addition to a semicircle and an inclined straight line, a spur in the high frequency domain starts appearing and finally it takes the shape of a depressed semicircle passing theough origin. At lowest temperatures, an inclined straight line disappears. A similar trend is observed for all composite systems under investigation. It is observed that the dwell time of less than 40 minutes, is not sufficient to attain the thermal equilibrium in the sample and so less reproducible impedance data, whereas dwell time of more than 50 minutes gives reproducible results. Thus the impedance was measured at the end of each dwell time of 60 minutes. The impedance data of all samples, at three different temperatures, are displayed in Table - 1. The disappearance of an inclined straight line at lowest temperatures is due to the lower limit of an applied field frequency to 5Hz. Furthermore, absence of high frequency semicircular arc at higher temperatures may be due to the upper frequency limit of 13 MHz of impedance analyzer.

Since aluminum foil at the electrolyte surface acts as irreversible electrodes for Li+, an inclined straight line in the low frequency domain is vividly due to electrode-electrolyte interface[21]. On the other hand, semicircular arcs at higher frequencies are as a result of the passage of electric current through the specimen[22]. The presence of two discernible depressed semicircular arcs suggests two prominent conduction meachanisms in the materials. In ion conducting specimens prepared from sintered powders, an experimental impedance obviously contains contributions from the intragrain and intergrain. From the the recent developments in the understanding of polycrystalline conductors[15,22], the intragrain conduction process can be attributed to two effects: (i) conduction due to mobility of ions parallel to interface in the highly disordered space charge region (σ) and (ii) conductivity as a result of ion transport in an iterior of grain (σ_g), along with an intergrain conduction across the interface denoted as (σ^+). The conductivity as a whole in such systems is a complex superposition of series and parallel contributions.

There would be many models to manifest the presence of two depressed semicircles in the complex impedance plane for pure polycrystalline Li_2SO_4. In the simplest case, here we have

Table. 1 Impedance data for Li_2SO_4: ABO_3 composites

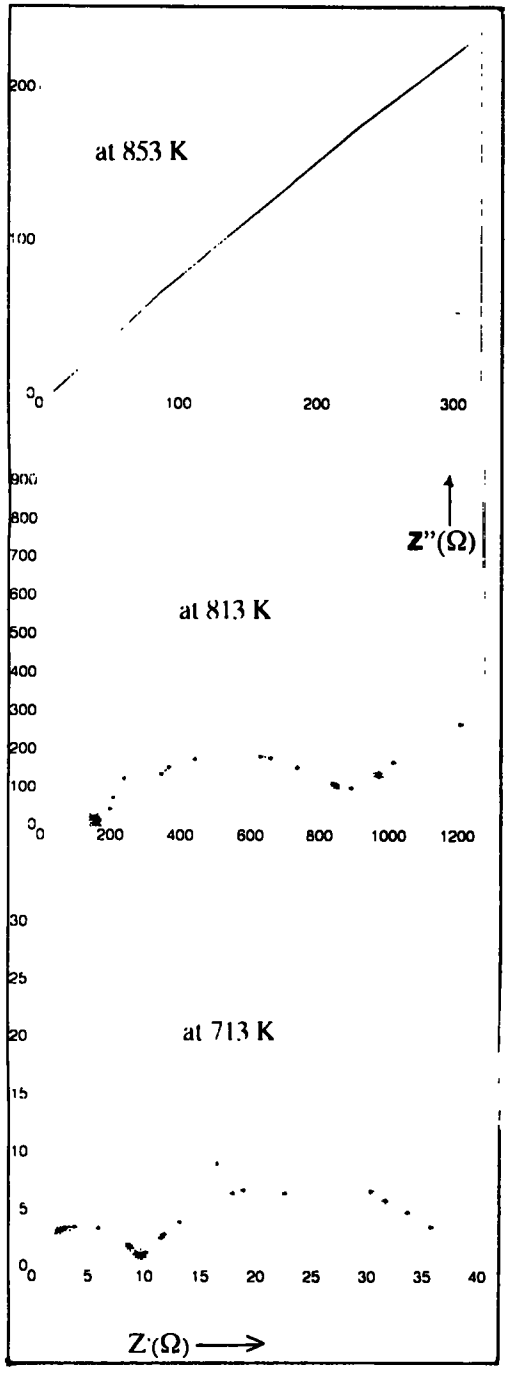

Sr. No.	Comp. (Wt%)	Temp. (K)	N	α_1	α_2	R_{b1} (ohm. cm)	R_{b2}
			Li_2SO_4:$BaTiO_3$				
		813	1	32		0.03	
1.	90:10	673	2	27	17	0.05	2.86
		613	2	23	06	24.59	4.08
		813	1	32		0.03	
2.	80:20	673	2	12	25	0.65	1.08
		613	1			3.59	
		813	1	30		0.016	
3.	70:30	673	1	22		2.43	
		613	1	25		14.72	
			Li_2SO_4:$KNbO_3$				
		813	1	17		0.17	
4.	90:10	673	2	5	18	0.20	0.36
		613	1	5		2.5	
		813	1	5		0.003	
5.	80:2	673	1	6		0.21	
		613	1	10		2.29	
		813	1	24		0.020	
6.	70:30	673	2	8	0.26	3	0.29
		613	1	10		2.733	
			Li_2SO_4:$LiNbO_3$				
		813	1	31		0.050	
7.	90:10	773	1	23		0.662	
		613	1	24		8.276	
		813	1	30		0.023	
8.	80:20	673	2	16	15	0.37	1.066
		613	1	21		3.08	
		813	2	28	27	0.019	0.057
9.	70:30	673	1	19		5.186	
		613	1	13		8.547	
2							
			Li_2SO_4:Al_2O_3				
		813	st line				
10.	80:20	673	st line			0.16	
		613	1	4		2.937	

N- Number of semicircles, R_{b1} - Real axis intercept of first semicircle, R_{b2} - Real axis intercept of second semicircle, α_1 angle of depression for first semicircle and α_2 angle of depression for second semicircle

Fig. 2 Cole-Cole plots at various temperatures

considered a brick wall model (Fig.3) instead of a very simple arrangement of squares suggested by Maier[15] so as to account for the above described conduction proceses. According to the space charge theory, the interfacial surface reaction increases the interstitial defects in one grain and vacancies at the regular site of its counterpart forming a space charge layer adjacent to the interface[15]. It is well known that the defect density in the space charge layer decreases exponentially in the direction of interior of the grain[14-16](Fig.4) characterised by Debye length,

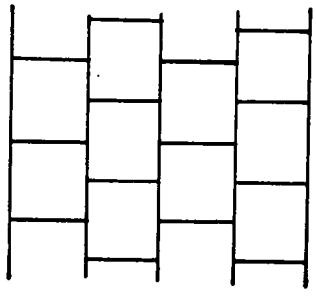

Fig. 3 Schematic presentation of compositions

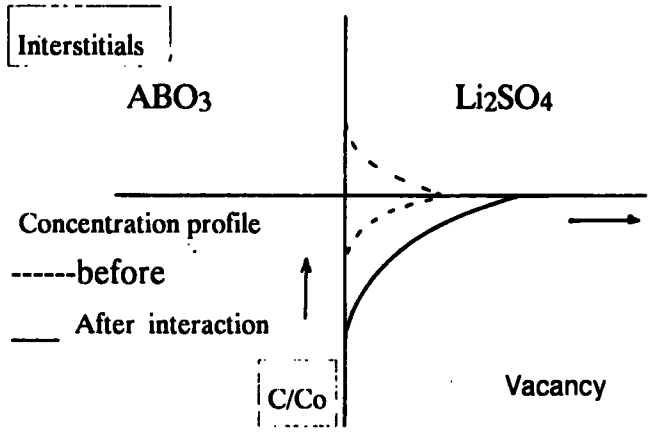

Fig. 4 Variation of defect concentration at the interface

$$\lambda = \sqrt{\frac{\varepsilon\varepsilon_0 kT}{2e^2 c\alpha}} \quad \text{----------} \quad (1)$$

Consequently, an expected ion current densities within the grain is extremely high close to interface (shown by continous lines in Fig.3) as compared to as one goes to the interior of the grain (depicted by dashed lines) constituting intragrain conduction i.e, $\sigma 1 = \sigma // + \sigma_g$ (where,$\sigma_1 = 1/Z_1$). At the end of each grain, ions migrate across the interface and enter into the adjacent grain resulting into intergrain conduction i.e.,$\sigma^{\perp}(\sigma^{\perp} = \sigma_2 = 1/Z_2)$. The details of Z_1 and Z_2 are discussed latter. The . In addition to the defects, in highly disordered space charge region the number of vacent sites are more than the available ions to fill them. Thus during the transport after a forward hop of mobile ion in the direction of applied electric field leaving behind a equivalent vacancy, there is a finite probability of backward jump. Moreover, the small inhomogeniety within the sample lead to a shortest and longest relaxation times. Both these phenomena limits the low and high relaxation time i.e. distribution in relaxation times (non-Debye type) is given by

$$Z(\omega) = Z(\infty) + \frac{Z(0) - Z(\infty)}{1 + (j\omega\tau)^p} \quad \text{----------} \quad (2)$$

Where $Z(\infty)$ and $Z(0)$ are limited values of $Z(\omega)$ whenω changes to '∞' from '0' respectively and 'τ' is known as the mean relaxation time deduced from the loss peak frequency. 'p' is an empirical measure of the departure from the ideal debye model. This leads to a depressed semicircle (center lying below real axis) and the angle of depression $\theta = p\pi$. Thus the impedance for intragrain transport is given by

$$Z_1(\omega) = \frac{Z^{||}(\omega) Z_g(\omega)}{Z^{||}(\omega) + Z_g(\omega)} \quad \text{-------} \quad (3)$$

where,

$$Z^{||}(\omega) = Z^{||}(\infty) + \frac{Z^{||}(0) - Z^{||}(\infty)}{1 + (j\omega\tau^{||})^{P^{||}}} \quad \text{and} \quad Zg(\omega) = Zg(\infty) + \frac{Zg(0) - Zg(\infty)}{1 + (j\omega\tau^g)^{p^g}}$$

Similarly,

$$Z_2(\omega) = Z^{\perp}(\omega) = Z^{\perp}(\infty) + \frac{Z^{\perp}(0) - Z^{\perp}(\infty)}{1 + (j\omega\tau^{\perp})^{p^{\perp}}} \quad \text{-----} \quad (4)$$

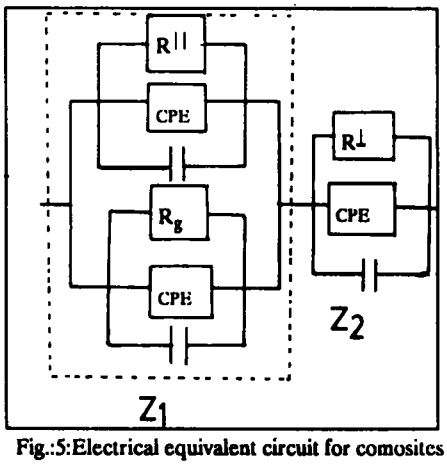

Fig.:5:Electrical equivalent circuit for comosites

Thus the total impedance of the composites under study (excluding electrode effect is given by)

$$Z_T(\omega) = \frac{Z^{||}(\omega) Z_g(\omega) + Z^{\perp}(Z^{||}(\omega) + Z_g(\omega))}{Z^{||}(\omega) + Z_g(\omega)}$$

where, $Z_T(\omega) = Z_2(\omega) + Z_1(\omega)$ ------(5)

The experimental valuesa of θ, $Z_{1(0)}$ and $Z_{2(0)}$ are given in Table-1. The entire conduction process could be represented by a simplified electrical equivalent circuit as shown in Figure 5. Two parallel combinations of resistors and capacitors as depicted

in figure 2c represent the intragrain conduction (circuit enclosed by dashed rectangle) and a parallel combination of resistor and capacitor in series with earlier one accounts for intergrain conduction. The CPA branch included in each sub-circuit takes care of small variation in the current densities in each case. Such a conduction process is obviously expected to give two depressed semicircles in the complex impedance plane.

3.2 Temperature and composition dependent conductivity

In any electrochemical device, the total conductivity of the sample (intra + intergrain conductivities) is important. The total conductivity of each sample (excluding electride-electrolyte interface) has been determined from the real axis intercept of second semicircle. Arrhenius plots for Li_2SO_4:$LiNbO_3$ composites depicted in Fig. 6 clearly indicate change over in the conduction mechanism. Almost a simialr trend is seen for $KNbO_3$ and $BaTiO_3$ dispersed systems. It is worth mentioning here that the change in slope of Arrhenius plots for pure Li_2SO_4 is also observed by Kimura and Greenblat[23] and Tilak et al[24]. Tilak et al have attributed it to changeover conduction mechanism from extrinsic to intrinsic (while heating) due to presence of insitu impurity (Low grade chemicals)[24]. Since the ingredients used in the present investigation are of high purity (AG Fluka Switzerland), the possibility of changeover mechanism as a result of

Table-2: Activation energy (eV) at high and low temperature regeions.

Compositions	E_1	E_2
pure Li_2SO_4	1.773	0.924
90Li_2SO_4:10$LiNbO_3$	2.222	0.924
80Li_2SO_4:20$LiNbO_3$	1.749	1.432
70Li_2SO_4:30$LiNbO_3$	2.018	1.503
90Li_2SO_4:10$KNbO_3$	2.828	1.503
80Li_2SO_4:20$KNbO_3$	2.359	1.365
70Li_2SO_4:30$KNbO_3$	2.263	1.408
90Li_2SO_4:10$BaTiO_3$	2.435	1.88
80Li_2SO_4:20$BaTiO_3$	1.987	1.045
70Li_2SO_4:30$BaTiO_3$	1.920	1.140

E_1 and E_2 are activation energies at high and low temperatures respectively

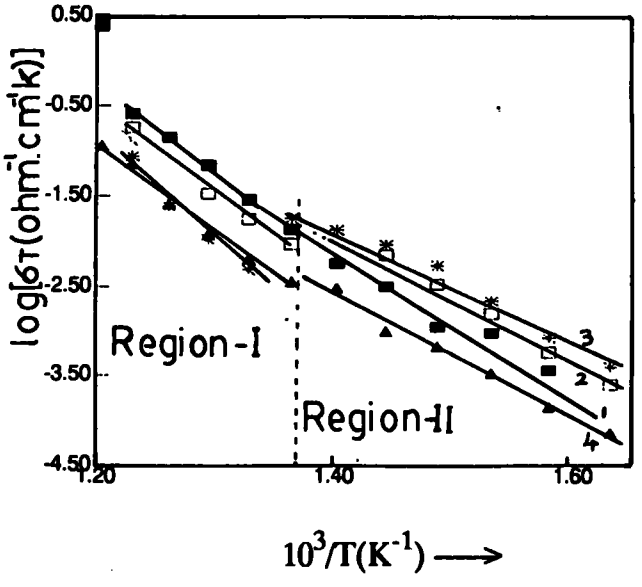

Fig. 6 Arrhenius plots for $LiNbNO_3$ dispersed Li_2SO_4

small impurity is probabaly ruled out. Instead, the recent theory on space charge region (disperse phase theory) suggests that the change in slope in Arrhenius plots of monocomponent system is due

to changeover mechanism from surface (surface percolation) to bulk (through the grains) conduction. Maier and Reichert have also observed similar results for polycrystalline solid electrolytes[25]. Thus, the entire temperature range of investigation is divided into two regions: (i) bulk conduction region (where intra-and inter-grain ion migration governs the conductivity and (ii) space charge conduction (ion migration along and across the space charge region leads to the ionic conductivity). The values of 'log', and 'E_a' for both the regions (E_1 and E_2) obtained using Arrhenius equation.

$$(\sigma T) = (\sigma T)_0 \exp.(-E_a/kT) \text{ ------- } (6)$$

are presented in Table2. Evidently, conductivity of ferroelectric dispersed Li_2SO_4, in geenral, decreases in region-I. On the other hand, a considerable enhancement in conductivity is seen in the space charge conduction region.

Since the ferroelectric insulating particles are insouble in Li_2SO_4 all compositions are two phase mixtures. It is well known that the space charge effect vanishes at higher temperature. Obviously, the ferroelectric dipersed particles act as ionically non-conducting entities which hinder the intergrian ion mobility, leading to overall decrease in conductivity and rise in activation energy as clearly seen from the Table-2. On the other hand, at low temperature the interaction at feroelectric/Li_2SO_4 interface is analogous to that at the moderate ion conductor/insulator interface which gives rise to space charge layer. Extending the similar analogy here, the expected surface reactions are:

$$M_{Li} + V_A = Li_A + V_{Li} \text{ ----- I}$$
$$M_A + Vi = Mi + V_A \text{ ----- II}$$

Where 'A' and "M" indicate the interface site and regular lattice site. The former (attractive interaction) reaction has a consequence that the Li ion would be sucked out of Li_2SO_4 volume and vacancy concentration is enhanced near the interface.

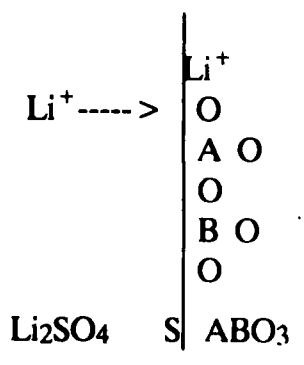

Fig. 7 Interface charge transfer mechanism according to reaction-II. A and B are cations and S-interface.

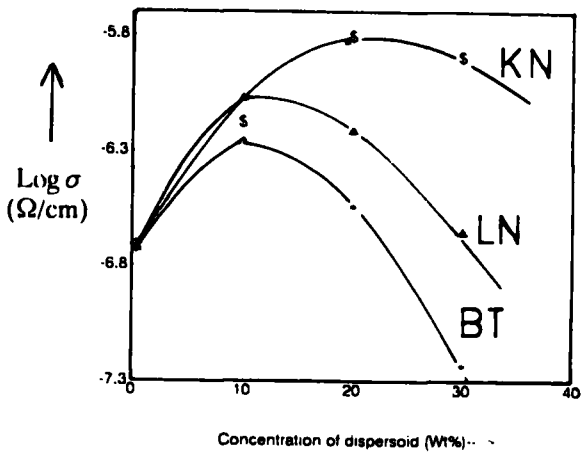

Fig. 8 Variation of log σ with ABO_3 concentration.

However, the latter (repulsive interaction) reaction would drive Li ion into Li_2SO_4 interstitial sites therby nehancing the interstitial ions. If we consider the latter case, a rise in interstitial ion would form clusters due to interaction amongst the mobile charge cations) in the defused space charge region inturn, reduces the ion mobility along the interface in want to nearby vacant site[26]. In contrast an order magnitute of increase in conductivity with a considerable decrease in activation enthalphy (Table-2) in region-II suggest an enrichment of vacancies (due to reaction-I) forming a diffused space charge layer near the interface. The charge transfer mechanism across the interface as per reaction - I is illustrated in figure 7. In this case, the surface oxygen ions are chemically at higher potential when compared to those ions inside the grains of ABO_3 (i.e. negatively charged surface oxygen ions) suck the mobile Li ions from adjacent Li_2SO_4 grain leaving vacancy at the interior of latter. Such a charge transfer reaction continues until chemical potential along with electrical potential attains the equilibrium, which in tern increases the concentration of Li+ vacancy forming a highly disordered space charge layer at the interface. The variation of relative vacancy concentration (C/C_0)(where C and C_0 are the defect concentration) with distance measured inside the grain from interface is shown in figure 4.

The variation of conductivity with dispersoid concentration is depicted in figure 8. Evidently the maximum enhancement is obtained at 20 wt % of ABO_3. This concentration dependent conductivity is completely different to those of PZT[18] and $BaTiO_3$ dispersed NZS[19]. As the concentration of sidpersoide Li_2SO_4 increases more surface percolating pathways are generated theerby increasing the overall conductivity. The maximum conductivity at 20 wt % of ABO_3 is due to the percolation thershold[27]. A closer look at Fig. 8 reveals that the enhancement in conductivity is achieved due to the dispersion of $KNbO_3$(KN), $LiNBO_3$(LN) and $BaTiO_3$ (BT) in decending order, i.e. $\sigma_{KN} > \sigma_{AN} > \sigma_{BT}$. It is worth mentioning here that the KN and LN at 603K remain in the ferroelectric phase whereas, BT undergoes a ferroelectric to paraelectric phase transformation at 393K. Obviously, the ferroelectric state has higher relative permittivity as compared to that of paraelectric state. Furthermore, it is found that ε(KN)1450[27] > ε(LN)90[28] > εBT around 603K. Since the surface charge density is higher in case of KN than those of LN and BT, the interaction in the former case is more pronounced than in the latter. Hence, the space charge layer due to KN dispersion is highly disordered and give rise to high conductivity.

4. CONCLUSION

Complex impedance spectroscopy is found to be a very useful tool for investigating the conduction mechanism in composite solid electrolytes. The ferroelectric materials give a considerable enhancement in the ionic conductivity. The highest conducting sample may be useful for electrochemical device applications.

ACKNOWLEDGEMENT

The authors are thankful to BRNS, Bombay (INDIA) for providing financial assistance to carry out the work.

REFERENCES

1. Kvist, A. and Lunden, A., *Z.Naturforch.* **22a**, 235(1965).
2. Deshpande, V.K. and Singh, K., *Solid State Ionics*, **6** 151 (1982).
3. Singh,K. and Deshpande, V.K., *Solid State Ionics*, **7**, 295 (1982).
4. Singh,K. and Bhoga, S.S., *Solid State Ionics*, **39**, 205 (1990).
5. Singh K., *Solid State Ionics*, **28/29**, 1371 (1988).
6. Lunden,A., Schroeder,K. and Ljungmark, H., *Solid State Ionics* **28/29**, 262 (1988).
7. Uvarov, N.F., Shivastava, O.P. and Hairetdinove, E.F., *Solid State Ionics*, **36**,39 (1989).
8. Liang, C.C., *J. Electrochem. Soc.* **120**, 1289 (1973).
9. Maier,J., J.Phys. *Chem. Solids*, **46**, 309, (1985).
10. Khala,M., Makyta,M., Levasseur,A., and Hagenmuller,P., *Solid State Ionics*, **15**, 163 (1985).
11. Poulsen,F.W.," *Transport-Structure relation in fast ion and mixed conductors*", Eds. F.W. Poulsen, N.H. Andesen, K. Clausen, S.Skaruup and O.T. Sorense, RISO, National Lab. Roskild (1985)p.67
12. Jow,T. and Wagner, J.B. Jr., *J.Electrochem Soc.* **126**, 1963 (1979).
13. Kliewer, K.L. and Keohler, J.S., *Phys. Rev.A*, **140**, 1226(1965).
14. Maier J., *J. Electrochem.Soc.* **134**, 1524 (1987).
15. Maier J., Bur. Bnsenges.*Physik. Chem.* **89**,355 (1985).
16. Maier J., Bur. Bnsenges.*Physik. Chem.* **90**, 29 (1986).
17. Singh, K., *Bull. Mater. Sci.* **9**, 355 (1987).
18. Saito, Y. Asai, Y., Ado, K. and Nakamura, O., *Mat Res.Bull.***23**, 1661 (1988).
19. Saito, Y., Mayne,J., Ado,K., Ymamoto,Y. and Nakamura,O., *Solid State Ionics*, **40/41**, 72(1990).
20. Singh, K., and Bhoga, S.S., *J. Mat. Sci.* **25**, 2520 (1990).
21. Singh, K., and Bhoga, S.S., *J. Electrochem. Soc.* **137**, 1970 (1990).
22. Singh, K., *Solid State Ionics*, **66**, 5 (1993).
23. Kimura,M. and Greenblatt,M., *Mater.Res.Bull.* **19**, 1653(1984).
24. Tilak,A.V.N. and Shahi,K., *Solid State Ionics*, **24**, 121 (1987).
25. Maier,J. and Reichert, Bur., Bunsenges, *Physik Chem.* **90**, 666 (1986).
26. Singh, K., and Bhoga, S.S., and Wachasundar, S.D., *Appl.Phys A* **55**, 493(1992).
27. Shirane, G., Jona, F and Pepivisky, R, *Proc IRE.*, **43**, 1738 (1955).
28. Deshmukh, K.G. and Singh,K., *J. Pure Appl. Phys.* **14**, 121(1976).